SLAC-PUB-15118

The SLAC P2 Marx

Mark A. Kemp[1], Andrew Benwell[1], Craig Burkhart[1], David MacNair[1], Minh Nguyen[1]

[1]SLAC National Accelerator Laboratory, Menlo Park, CA , 94025 USA

ABSTRACT

A proposed high energy physics accelerator, the International Linear Collider, will require greater than five hundred rf stations. Each station is composed of a klystron driven by a modulator. Recently, the SLAC P2 Marx was designated the baseline modulator for the ILC. This paper describes some key features of this modulator and presents recent experimental results.

Index Terms — **Power Modulators, Accelerators, Marx Banks**

1 INTRODUCTION

The International Linear Collider is a large, multi-national program with technology challenges in the rf accelerator system [1]. SLAC National Accelerator Laboratory (SLAC) has been researching one aspect of this accelerator, the klystron modulator. The first generation modulator, the P1 Marx, has been designed and built and is currently undergoing lifetime testing [2]. Both building upon the lessons learned during the P1 Marx project and incorporating new concepts, the SLAC P2 Marx (P2 Marx) project was initiated [3-10]. This is the latest modulator in a solid-state Marx program at SLAC which dates back over twelve years [11].

The basic Marx topology operates upon the principle of charging capacitors in parallel and discharging them in series. The maximum voltage across a given cell switch is the same as the charging voltage. Therefore, by stacking up many stages, low voltage switching can be used to generate high voltages. Given the parameters of the ILC modulator, shown in Table 1, a solid-state Marx modulator was determined to be a viable alternative to the previous baseline, the bouncer modulator [12].

This paper is a summary of some of the recent progress made on the P2 Marx. First, an overview of some aspects of the design are highlighted. Second, some experimental results of the full modulator are discussed. Finally, potential future applications of the technology are introduced.

Table 1. ILC klystron modulator parameters.

Output Voltage	120 kV
Output Current	140 A
Pulse Width	1.6 ms
Pulse Repetition Frequency	5 Hz
Average Power	134 kW
Output Pulse Flat-top	±0.5%
Energy Deposited into Klystron During a Gun Spark	<20 J

2 DESIGN

The basic building block of the Marx modulator is the cell. Much of the detailed operation of the cell is described elsewhere [10], so only the main characteristics are highlighted here. A simplified schematic of the cell is shown in Fig. 1. There is a main storage capacitor, C1, and a correction storage capacitor, C2. These capacitors are charged up to -4kV and -1kV respectively. The main fire switch, Q1, and the main charge switch, Q2, are implemented using a single, 6.5kV IGBT half-bridge. The correction fire, Q3, and recovery, Q4, switches are a 1.7kV IGBT half-bridge. Charging is accomplished through 6.5kV diodes.

The basic operating principle of the cell is that it produces a “square” output pulse. The RC droop of C1 is compensated by the correction portion of the cell. The Q3 switching is determined by a closed loop, pulse width modulation (PWM)

Table 2. P2 Marx cell and modulator parameters.

Cell Weight	< 50 lb
Cell Dimensions (inc. shield) (WxDxH)	13.75”x29.5”x8”
Cells Per Modulator	32
Minimum Cells for Full Output	30
Modulator Dimensions (WxDxH)	9’x5’x8’

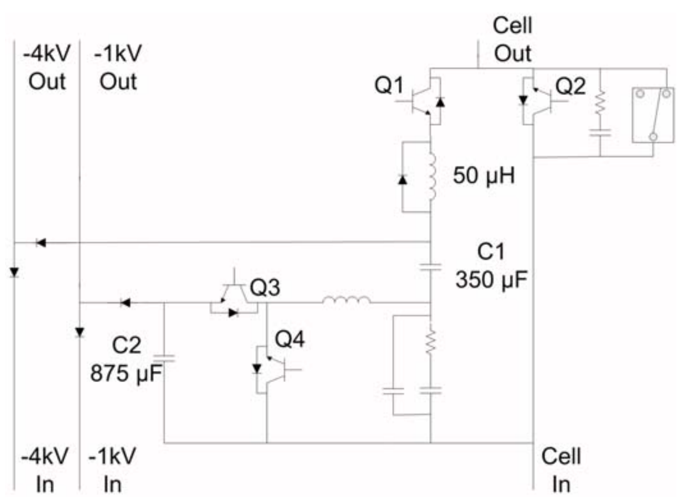

Figure 1. P2 Marx single-cell simplified circuit schematic.

Presented at the 2012 International Power Modulator and High Voltage Conference
San Diego, CA , June 3-7, 2012

Work supported by US Department of Energy contract DE-AC02-76SF00515.

scheme. This switching results in a ramp-up of the voltage across the filter capacitance which offsets a corresponding ramp-down of C1. After the pulse, Q4 is chopped to recover the filter energy back to C2. Stated differently, the correction portion of the cell is a "buck" converter during the pulse, which transfers energy from C2 to the load and charges the filter capacitance. After the pulse, a "boost" converter transfer the energy from the filter capacitance back to C1 [10].

The modulator is controlled using a hierarchical control scheme, diagramed in Fig. 2 [3]. Each cell is controlled by a "hardware manger." This FPGA-based platform distributes the trigger to the IGBT gate drives, digitizes cell diagnostics, controls the cell relays, and provides the state control of the cell. Through a fiber giga-bit Ethernet link, each hardware manger is connected to a ground-level Ethernet switch. This switch is also the interconnection point for a power supply controller, a PC, and the "application manager." The application manager distributes triggers to all the cells, incorporates external interlocks, digitizes global diagnostics, and controls the state of the modulator. Developments are presently underway to migrate the functionality presently associated with the PC and the application manger to a VME processor running an EPICS IOC.

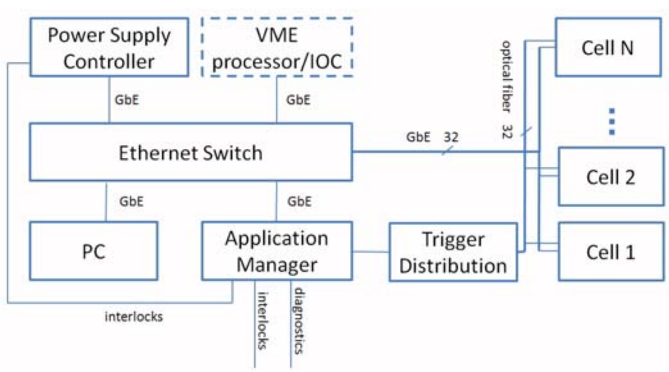

Figure 2. Controls block diagram for the P2 Marx modulator. Presently, a PC is used to control the modulator state, and view and store diagnostics. A planned upgrade is to migrate this functionality to a VME/EPICs based system.

Figure 3. Photograph of the P2 Marx modulator.

The full modulator is made up of 32 cells. Up to two of these cells can fail without inhibiting the modulator from producing the specified output pulse. The modulator uses all air insulation and cooling for the high voltage cells. Heat is removed from the modulator enclosure via an air/water heat exchanger. Blowers circulate air through ducts which direct flow across the cell heat sinks. The enclosure is intended to be air-tight such that minimal waste heat is rejected to the ambient. A photograph of the modulator is shown in Fig. 3.

One feature of the Marx topology is the fact that, at the cell level, the components and electronics are all referenced to "cell low." An electrostatic cell shield is electrically connected to each cell. This shield floats up and down as the Marx erects. Any C*dv/dt currents associated with the high-voltage Marx transients are shunted through this shield. All electronics and sensitive components only "see" the local cell voltage. Therefore, the cell is inherently noise-immune and is not susceptible to deleterious effects due to fast transients.

Efficiency is particularly important for the ILC klystron modulator because of the large overall power consumption of the accelerator. Small increases in the efficiency can potentially make a large overall difference. The calculated efficiency for components in a typical Marx cell is shown in Fig. 4. Depending upon the position of a cell within the Marx stack, the loss distribution will change. For example, the lowest cell in the Marx will have the highest amount of losses associated with charging currents. The top cell will have nearly zero. Calculations of modulator efficiency show the overall Marx efficiency to be ~95%. Measurements to confirm this calculation are ongoing.

3 EXPERIMENTAL VALIDATION

As of the date of this publication, the Marx has been tested into a water load. The modulator is presently being transported to a different facility to operate into a 10 MW klystron. Results in this section are for water load operation.

The measured modulator pulse is shown in Fig. 5. This was obtained with a commercial, 20 MHz, high-voltage probe. A secondary measurement was also obtained by summing the individual voltage dividers in each of the cells. While the cell voltage dividers do not account for cell-cell bus losses, the

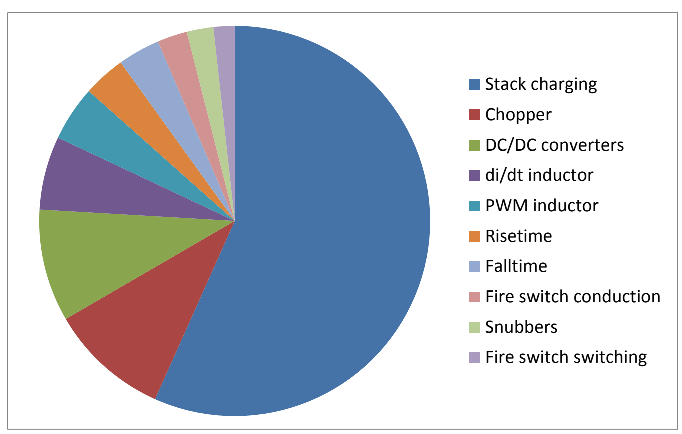

Figure 4. Calculated distribution of losses for a typical P2 Marx cell.

two measurements agree to less than 0.5%. As shown, the rise and fall times of the pulse are less than 10 us, and there is no pre-and post-pulse artifacts from the modulator.

Figure 6 illustrates the flat-top portion of a typical pulse. To take advantage of the deterministic nature of the ripple from the individual cells, correction portions of the cells can be appropriately staggered in time to result in a minimal overall modulator ripple. In Fig. 6, the blue trace was measured when the PWM timings of all the cells were all synchronized. As shown, there is a sinusoidal pattern modulated on top of the waveform. The red trace shows when the PWM portions of the cells are staggered. Here, the ripple is minimal with a magnitude of less than +/-0.05%.

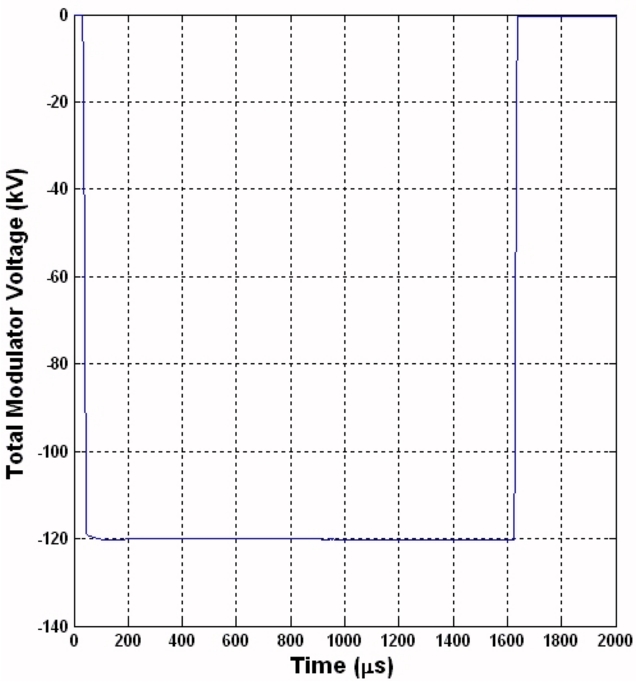

Figure 5. Measured modulator output voltage into a water load.

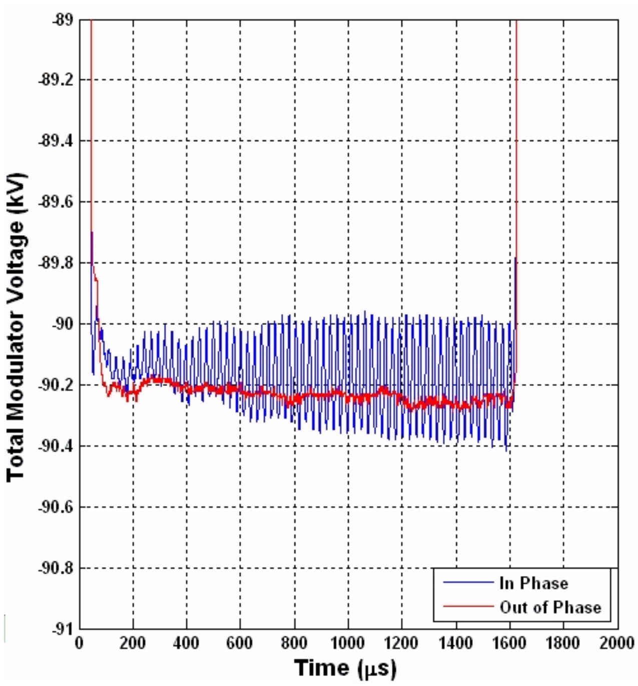

Figure 6. Measured output voltage of the modulator operating into a water load. Flat-top portion of cell is highlighted. The blue trace shows when the cell PWM timings are synchronized "in-phase" and the red trace shows when they are placed out of phase.

One challenging parameter for many klystron modulators is fault susceptibility. In particular, a klystron gun spark is a prevalent condition. In addition to not damaging the modulator, the energy deposited in the klystron during an arc event must be less than 20J.

To simulate a klystron arc event, a self-break spark gap was placed in parallel with the water load. Sized and spaced appropriately, the gap will break down at the maximum Marx voltage. A typical arc-down event is shown in Fig. 7. After the modulator is at full voltage, the arc occurs at ~78 μs. After the modulator protection circuits detect the arc event, the fire IGBTs are opened, and after a <10μs delay, the charge IGBTs are closed. As shown, the current through the arc decreases. Greater than fifteen arc events were survived in the laboratory without sustaining modulator damage.

An additional safety feature for the Marx was implemented to ensure the energy in the cell is not transferred to the load during an arc. If the fire IGBT fails to inhibit current flow to the load, the closure of the charge switch will result in the capacitor energy remaining contained within the cell. Unfortunately, this results in damage to the charge switch. However, a single IGBT failure is preferable to klystron damage. This protection mechanism prevents a single-point failure from resulting in klystron damage

Relating the self-break arc data to energy deposited within a

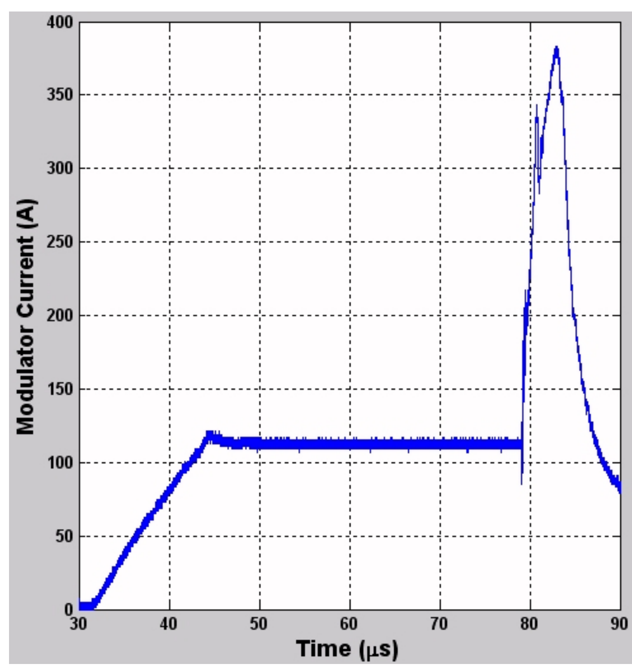

Figure 7. Measured modulator current before and during an arc. At ~78 μs a self-break spark gap across the load closes. This test was performed at 120kV modulator output voltage.

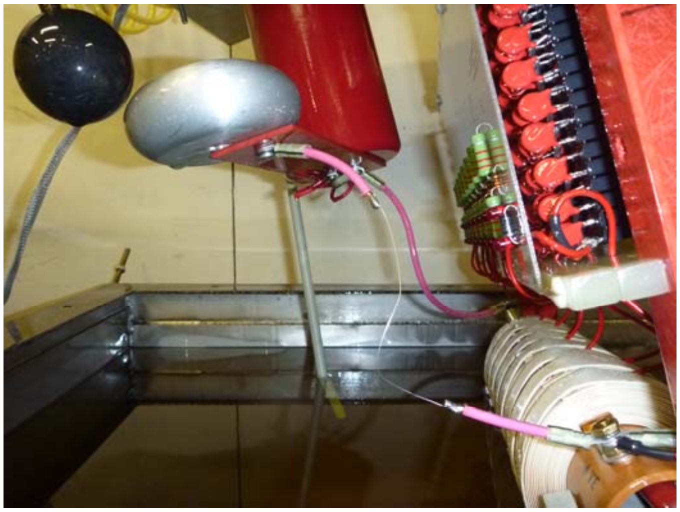

Figure 8. Measured modulator current before and during an arc. At ~78 µs a self-break spark gap across the load closes. This test was performed at 120kV modulator output voltage.

klystron is not necessarily straightforward [13]. One way to do so is to assume a voltage for a typical klystron arc. An arc voltage less than 100V is reasonable. With an assumed arc voltage, the energy transfer requirement can be also thought of as a charge transfer requirement. Hence, integrating under the current trace during the arc event will confirm low-enough charge transfer.

Another method to use is the "wire test." An appropriately-sized wire is placed in series with the spark gap. If too much energy is deposited in the wire, it will fuse open. For an assumed 100V arc and 20J, a 10 cm-long, 30 ga copper wire is used [14]. A photograph of this setup is shown in Fig. 8. Indeed, during all of the arc-down events, this wire did not fuse. This can be used as a secondary data point to illustrate that the P2 Marx will not transfer excess energy to the klystron during a fault.

4 SUMMARY

The P2 Marx is presently being transported to another facility for lifetime testing. Here, we will gain understanding of how the Marx performs into a klystron load and gain experience operating the Marx for longer periods. Long term plans include the possibility of using this rf station for L-band technology demonstration at SLAC.

While the Marx was designed with the ILC in mind, the topology can be readily applied to several different applications. We are currently evaluating the use of the topology for ESS, CLIC, and upgrades for systems at Fermi National Accelerator Laboratory. Because of the modular nature of the cell and the robustness of the control system, many different combinations of series and parallel operation are possible along with different load currents and pulse shapes.

ACKNOWLEDGMENT

Work supported by Department of Energy contract DE-AC02-76SF00515. SLAC-PUB-15118.

The authors recognize the contributions of Patrick Shen, Chris Adolphsen, Chuck Yee, John Hugyik, Joe Olszewski, Wanda Gorecki, Chaofeng Huang, Koen Macken, David Anderson, and Jeff Olsen.

REFERENCES

[1] N. Phinney, *et al.*, "ILC reference design report volume 3-accelerator,"arXiv:0712.2361, 2007.

[2] C. Burkhart, *et al.*, "P1-Marx modulator for the ILC," 2010 IEEE Power Modulator Conference, Atlanta, GA, 2010.

[3] D. MacNair, *et al.*, "SLAC P2 Marx control system and regulation scheme," PAC'11, New York, March 2011.

[4] M.N. Nguyen, *et al*., "Compact, intelligent, digitally controlled IGBT gate drivers for a PEBB-based ILC Marx modulator," IPAC'10, Kyoto, Japan, May 2010.

[5] K. Macken, *et al.*, "A hierarchical control architecture for a PEBB-based ILC Marx modulator," in *Proc. IEEE Int. Pulse Power Conference*, Washington, DC, June 2009

[6] A. Benwell, *et al.*, "A prognostic method for scheduling maintenance on the P2-Marx modulator," 2010 IEEE Power Modulator Conference, Atlanta, GA, 2010.

[7] K. Macken, *et al*., "Towards a PEBB-based design approach for a Marx-topology ILC klystron modulator," PAC'09, Vancouver, BC April 2009.

[8] M.A. Kemp, *et al.*, "Status update on the second-generation ILC Marx modulator prototype," 2010 Power Modulator Conference, Atlanta, GA, 2010.

[9] M.A. Kemp, *et al*., "Design of the second-generation ILC Marx modulator," LINAC 2010, Tsukuba, Japan.

[10] M.A. Kemp, *et al.*, "final design of the SLAC P2 Marx klystron modulator," 2011 Pulsed Power Conference, Chicago, IL.

[11] A. Krasnykh, *et al.*, "A solid state Marx type modulator for driving a TWT," Power Modulator Symposium, 2000.

[12] H. Pfeffer, *et al.*, "A long pulse modulator for reduced size and cost," 21st Power Modulator Symposium, 1994.

[13] S.L. Gold, "Klystron gun arcing and modulator protection," SLAC-PUB-10435.

[14] J.T. Bradley III, *et al.*, "Test wire for high voltage power supply crowbar system," 1997 Pulsed Power Conference.